PROCEEDINGS OF SCIENCE

A Cosmic-Ray Propagation Model based on Measured Nuclei Spectra

Holger Motz[a,*]

[a] *Kanagawa University, 3-27-1 Rokkakubashi, Kanagawa, Yokohama, Kanagawa 221-8686, Japan*

E-mail: motz@aoni.waseda.jp

The cosmic-ray nuclei spectra feature breaks in their power-law shapes, with slight differences in the indices and in the break positions between the nuclei species. A model explaining these structural differences as propagation effects is presented, based on the hypothesis that the source spectrum from acceleration in supernova remnants is a common broken power law with exponential cut-off for all nuclei species. The observed structural differences in the spectra are instead attributed to soft breaks in the power-law rigidity dependence of the diffusion coefficient, as well as a spatial variation of the diffusion coefficient within the galaxy. Using a modified version of the numerical cosmic-ray propagation calculation code DRAGON and optimizing the model's input parameters in a random walk, it is shown that such a model can, within experimental uncertainty, explain various nuclei spectra and primary-secondary ratios measurements by the ISS-based experiments CALET (Calorimetric Electron Telescope) and AMS-02 (Alpha Magnetic Spectrometer), as well as the CRS (Cosmic Ray Subsystem) on the Voyager space-probes.

38th International Cosmic Ray Conference (ICRC2023)
26 July - 3 August, 2023
Nagoya, Japan

*Speaker

PoS(ICRC2023)068

1. Introduction

Using charged cosmic rays as messengers for the study of astrophysical phenomena such as supernovae and their remnants or potential signatures of dark matter annihilation or decay requires an understanding of their diffusive propagation throughout the galactic magnetic field, as it distorts the spectral information and largely negates any directional information. Concretely for this work the motivation is to obtain suitable propagation conditions for electron/positron cosmic rays in the GeV to TeV range for interpretation of CALET and AMS-02 data [1] and indirect dark matter search [2]. Since nuclei cosmic rays experience much less energy loss than electrons they have longer propagation distances and times, and their sources are distributed throughout the galaxy and over millions of years. At a SNR rate of a few per century, individual source positions and ages are less important for the observed nuclei spectra at Earth. Especially the relations between nuclei spectra can reveal propagation conditions, as the production of secondary cosmic rays depends on the amount of ISM encountered, and unstable nuclei and their decay products depend on the residence time. The observed nuclei spectra are power laws in general but their index changes with rigidity at several points, namely a softening at the order of 10 GV, followed by a hardening around a few 100 GV to 1 TV, and finally a softening at a few 10 TV. Discussed as causes for these features are breaks in the power-law rigidity dependence of the diffusion coefficient, spatial dependence of the diffusion coefficient, the properties of the source spectra and nearby sources, as well as combinations of these [3–8]. The indices and break positions in the spectra of the different nuclei species differ, which may be explained by nuclei species specific source spectra or propagation, or possibly by the contribution of secondary cosmic rays to the spectra. Species specific source spectra with a uniform diffusion coefficient are shown to produce a consistent explanation of the nuclei spectra using the numerical propagation calculation code DRAGON [8, 9]. Using also DRAGON (with custom modifications based on an earlier version of the code [10]), this work on the other hand aims to explain the current nuclei spectra measurements with as little complexity on the source side as possible, assuming a common source spectrum for all primary nuclei, instead tuning the rigidity and spatial dependence of the diffusion coefficient to achieve agreement with the data.

2. The Hypothesis

The model used in this work is founded on the hypothesis that all primary nuclei species have a common source spectrum, a power law with index γ_l below, and γ_i above the break at R_{bi} with softness s_{bi}, and with an exponential cut-off at R_{cut}. The spatial distribution of the sources is assumed to follow the model in Ref. [11] (standard choice in DRAGON), modulated with a spiral arm pattern with arm width w_{sa} Spectral differences between the nuclei species are attributed to propagation with a rigidity and position dependent diffusion coefficient as given by equation 1 and diffusive re-acceleration with Alfven speed v_a.

$$D(r,z,R) = D_0 \max\left\{e^{(r-r_n)/r_s}, 1\right\} \max\left\{e^{(z-z_n)/z_s}, 1\right\} \left(\frac{R}{R_0}\right)^{\delta_l} \left(1+\left(\frac{R}{R_{bl}}\right)^{\frac{\delta_l-\delta}{s_l}}\right)^{s_l} \left(1+\left(\frac{R}{R_{bh}}\right)^{\frac{\delta-\delta_h}{s_h}}\right)^{-s_h} \quad (1)$$

The diffusion coefficient softens from δ_l to δ at R_{bl} with softness s_l, then hardening again to δ_h at R_{bh}. It exponentially increases with galactic radius r and distance from the disk z, with constant central zones below $r_n = 2$ kpc, the galactic center, and below $z_n = 0.1$ kpc, the galactic disk. The motivation for introducing this spatial dependence is the assumption that the sources concentrated

in galactic center and disk cause the magnetic field turbulence which limits the particle diffusion speed, and that their influence should decrease with distance. The exponential dependence was chosen since it is smooth, avoiding instabilities in the numerical calculation occurring with step or linear slope functions. The central constant zones are introduced to avoid localized minima in the diffusion coefficient, especially at the observation point, the solar system. The conceptual idea is to create different propagation conditions for the nuclei species depending on how far they propagate out into the halo and back based on their nuclei mass and mass to charge ratio, with the expectation that the heavier nuclei would be confined to the inner regions with lower diffusion coefficient. However, since the model comprises 17 free parameters, no quantitative reasoning is done. Instead, the parameter space is explored by a random walk method attempting to find the best suitable model.

3. Calculation of Nuclei Spectra and Comparison to Data

The predicted nuclei spectra for one realization of the model determined by the 17 free parameters are the output of a calculation of the spallation network from a chosen heaviest nucleus (nickel in principle) to protons, with the additional calculation of antiprotons and lepton spectra used as part of the modeling in Refs. [1, 2]. A sufficiently fine spatial binning to properly reflect the spatial variation of source function and diffusion coefficient is necessary. Making use of the variable spatial binning option in DRAGON, the bin size is set to 0.05 kpc near the galactic plane in parameter z (galactic height), and in x and y near the solar system position (x=8.3 kpc, y=0, z=0) and the galactic center, increasing from these points in steps up to a 0.5 kpc base bin size in other regions of the Galaxy. The simulated diffusion zone extend 16 kpc from the galactic center in x any y, and 6 kpc in z. In this model, the diffusion zone height (L) is not a sensitive parameter since the escape of particles from the diffusion zone is determined by the outwardly increasing diffusion coefficient, and it was confirmed that 6 kpc is sufficiently large to have no significant impact on the results. The logarithmic binning in rigidity is set to a factor 1.1 between calculation points, covering the range from 1 MeV to 500 TeV, leaving a surplus margin on both sides (also at low energy end due to diffusive re-acceleration) to account for border effects. The calculated nuclei spectra are quantitatively compared to available experimental data, choosing one experiment's data where there is no agreement between different experiments measuring the same spectrum. For the mostly primary species, proton, helium, carbon and oxygen, the absolute spectral flux data is used. The comparison is restricted to above an energy of 5 GeV/nucleon to avoid inconsistencies from potentially time dependent solar modulation effects. The spectra measured by Voyager outside of the heliosphere are used at the low energy range without applying the correction for solar modulation. In detail, the used data-sets are:

- Proton flux from Voyager in the range 0.13 – 0.35 GeV [12]
- Proton flux from AMS-02 in the range 5 GeV – 1 TeV [13]
- Proton flux from CALET in the range 1 – 60 TeV [14]
- Helium flux from Voyager in the range 0.11 – 0.66 GeV [12]

- Helium flux from AMS-02 (in rigidity) in the range 11 GV – 3 TV [15]
- Carbon flux from CALET in the range 10 GeV – 2.2 TeV [16]
- Oxygen flux from CALET in the range 10 GeV – 2.2 TeV [16]

For the proton flux, the transition from the AMS-02 spectrum to CALET spectrum is set at 1 TeV, which is a characteristic energy above which the energy resolution of the magnet spectrometer declines, making the calorimeter the best suited experiment. In addition to the spectra of the primary nuclei, the following primary to secondary ratios are used in the fitting:

- Antiproton fraction from AMS-02 (in rigidity) in the range 5 – 450 GV [14]
- ^{3}He/^{4}He ratio from AMS-02 in the range 5 – 10 GeV [17]
- B/C ratio from AMS-02 in the range 5 GeV – 1.3 TeV [18]
- ^{7}Be/Be ratio in the range 0.25 – 0.85 GeV based on PAMELA data [19]
- ^{10}Be/^{9}Be ratio in the range 0.25 – 0.85 GeV based on PAMELA data [19]

The spectra obtained from DRAGON are fitted to the combined data by optimizing eight parameters: A normalization correction factor for each of the proton, helium, carbon and oxygen spectra, as well as four parameters (base potential Φ_0, the additional potentials Φ_{1+} and Φ_{1-} for positively and negatively charged particles, reference rigidity R_r) governing the rigidity and charge sign dependent force-field potential (inspired by Ref. [20]) for solar modulation correction given by

$$\Phi(R) = \Phi_0 + \Phi_{1\pm}\frac{1 + (R/R_r)^2}{(R/R_r)^3} \,. \tag{2}$$

The solar modulation correction is applied to each isotope's flux individually, then χ^2 for the combined flux is calculated. Similarly, ^{3}He and ^{4}He are converted independently to rigidity, then added up, for fitting of the AMS-02 helium flux data.

4. Scanning the Parameter Space

To obtain a set of source and propagation parameters matching the data best, the calculation and fitting to data described in section 3 is performed repetitively in a random walk procedure to explore the 17-dimensional parameter space. While the direct data fitting yields the total (summed up) χ^2 of all experimental data-points, this is not a suitable quality parameter for the overall model, since it puts strong focus on measurements with many data-points at the expense of those with few data-points (e.g. the Voyager data). Instead, the sum of logarithms of the p-values calculated from each experiment's χ^2, with the contribution of the worst fitting experiment doubled, was used to asses a data-sets fit quality and guide the random walk process. The algorithm to find and test new parameter sets combined a Markov-Chain random walk with gradient descent and interpolation/extrapolation from already calculated models. To reduce the required calculation effort, the model optimization was initially performed calculating and fitting the helium-proton (with antiproton) and oxygen-beryllium nuclei ranges separately, before combining them by calculating the silicon-proton range

parameter	D_0 [10^{28}cm^2/s]	R_0 [GV]	L [kpc]	v_a [km/s]	γ_l	R_{bi} [GV]	s_{bi}	γ_i	R_{cut} [TV]	w_{sa} [kpc]
value	**3.066**	4	6	**14.74**	**2.030**	**13.45**	**0.2285**	**2.858**	**30.12**	**0.6478**

r_n [kpc]	r_s [kpc]	z_n [kpc]	z_s [kpc]	δ_l	R_{bl} [GV]	s_l	δ	R_{bh} [GV]	s_h	δ_h
2	**10.7**	0.15	**4.50**	**0.2112**	**8.4373**	**0.0529**	**0.5141**	**913.5**	**0.3262**	**0.0018**

Table 1: Parameters of the best-fit reference model, see text for explanation. Values in bold font were obtained by the optimization, others are fixed values.

and finally confirming the result by calculating the full nickel-proton network. In the partial calculations, correction factors to the light nuclei spectra were used to account for the contribution of not calculated heavier nuclei, with the correction factors obtained by interpolating between a limited number of full (nickel-proton) calculations.

5. Best Fitting Propagation Model

Concluding the optimization procedure described in section 4 after no further improvement was observed for a signification number of trials, the parameter set with the best quality estimator was taken as the reference model presented in the following. The model's parameters are listed in table 1, the fit function compared to the nuclei spectra is shown in Fig. 1, and to the primary-secondary ratios in Fig. 2. The overall fit quality is $\chi^2 = 230$ with 290 degrees of freedom, and the p-value for each individual experimental result is 0.29 or larger.

6. Interpretation and Predictions

In the following, notable features of the model and the relation to other experimental results than those used in the optimization are discussed. The proton spectrum from CALET shows a sudden softening near 10 TeV, which is well reproduced by the exponential cut-off of the source spectrum at 30 TV. This softening is less pronounced in DAMPE's data[21], which otherwise agrees within error. In the AMS-02 helium spectrum, secondary ^{3}He contributes significantly in the rigidity range from 10 to 100 GV, changing the spectral shape as speculated by the initial hypothesis. The spectrum of helium in energy per particle (see Fig. 3) measured by DAMPE [22] was not considered in the optimization, but the model agrees within error. The spectrum recently published by CALET [23] features a steeper hardening and higher flux in the TEV region, which is not reproduced by this model. It will be investigated in future work if the model can be adapted to accommodate this measurement. The ratios of unstable beryllium isotopes are correctly reproduced, showing that the exponential increase of the diffusion coefficient with z results in the correct resident time of these nuclei. The spectral hardening in the nuclei spectra is explained by this model by the transition from diffusion coefficient index $\delta = 0.5141$ (coincidentally matching Kraichnan turbulence) to $\delta_h = 0.0018$. This strong break is counteracted by the exponential cut in the source spectrum which brings down the spectra near 10 TV. With δ_h near zero, the model predicts that the B/C becomes flat in the TeV region, which could be tested by future extensions of the data range. The model is found to be also in good agreement with the recently published CALET measurement [24] as shown in Fig. 2. The carbon and oxygen spectra measured by AMS-02 [25] show a discrepancy in

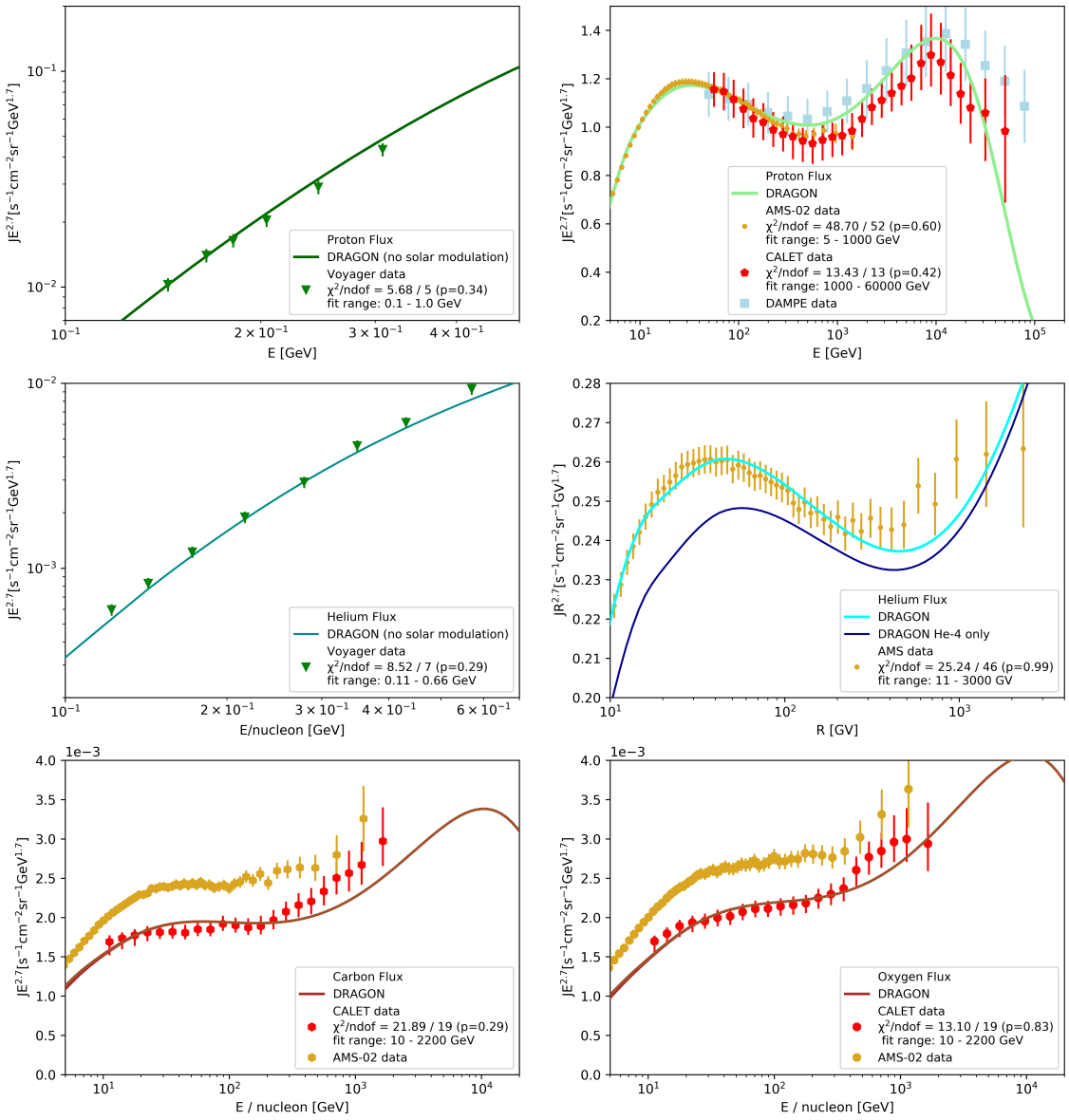

Figure 1: Comparison of the reference model to experimental nuclei spectra results, see legends for details and text for explanation.

normalization with the CALET data, but have a similar spectral structure. A separate optimization using the AMS-02 spectral data will be done in future work. The iron [26] and nickel [27] spectra measured by CALET are reproduced well if fitted with a scale factor for iron as an additional parameter, as shown in Fig. 3. Similar to carbon and oxygen, there is a normalization discrepancy with AMS-02 [28]. The model predicts a hardening of the iron and nickel spectra falling within error of the current measurements, but which may be resolved in the future.

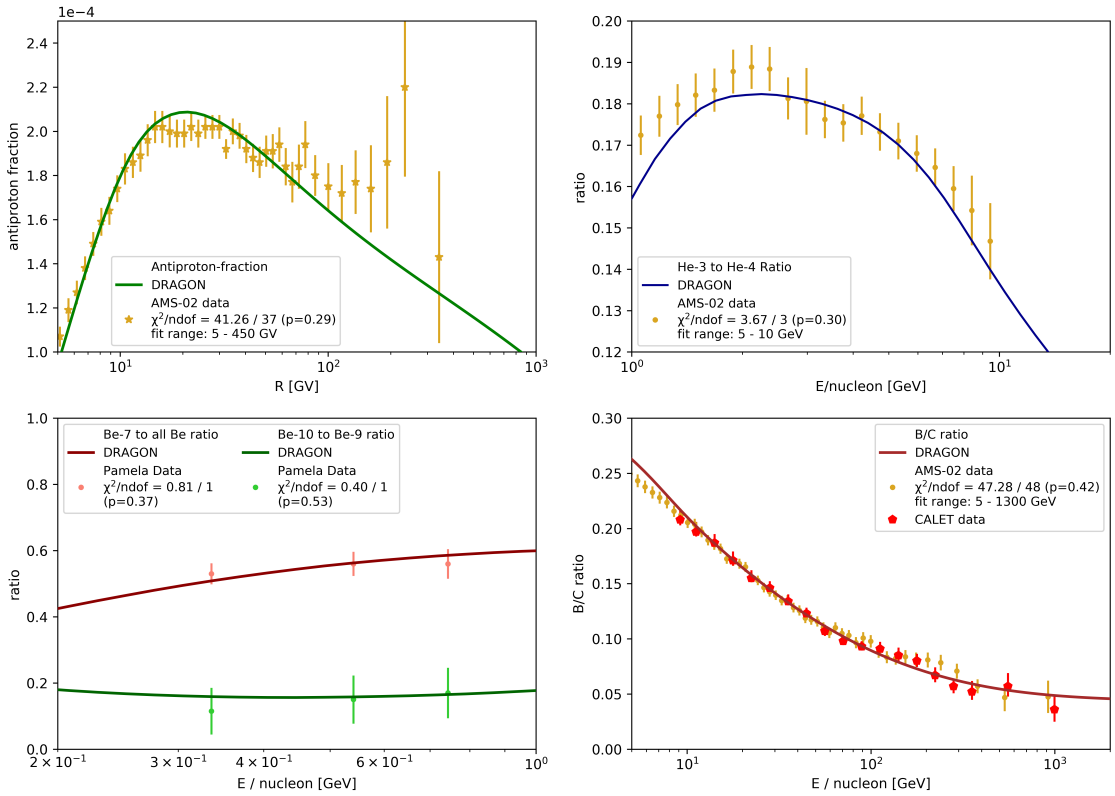

Figure 2: Comparison of the reference model to experimental primary to secondary ratio results, see legends for details and text for explanation.

7. Conclusion

The presented model with a common source spectrum for all primary nuclei shows that explaining current nuclei measurement data within experimental uncertainty based on propagation effects is possible. The differences in the spectral structures depending on the nuclei species could be caused by the propagation throughout the galactic halo with a diffusion coefficient which depends on both position and momentum. While the presented reference model is optimized based on the selected data-sets listed in section 3, it is planned to take recently published and future experimental results into account in a later revision.

Acknowledgments

This work was supported in part by JSPS Grant-in-Aid for Scientific Research (S) Grant No. 19H05608, and by JSPS Grant-in-Aid for Scientific Research (C) Grant No. JP21H05463.

References

[1] H. Motz, *PoS* **ICRC2023**, PCRD2 (2023).
[2] H. Motz, *PoS* **ICRC2023**, DM5 (2023).

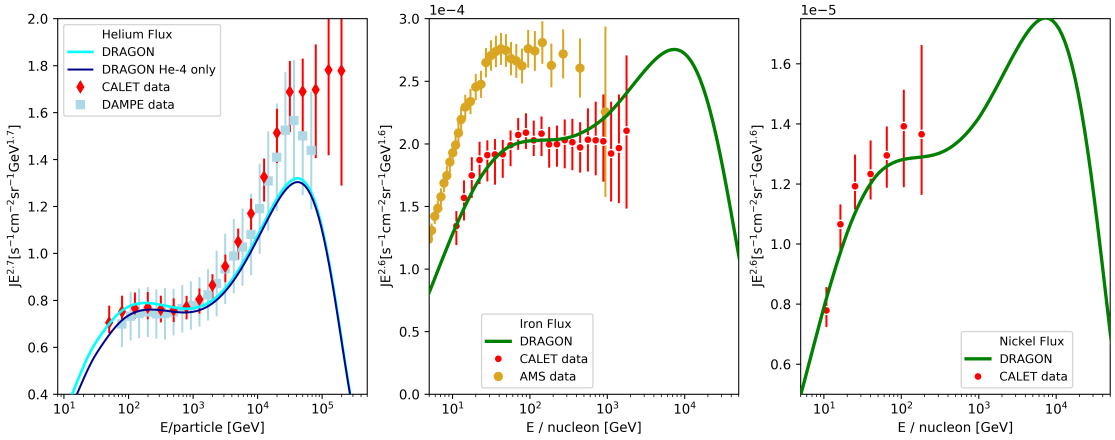

Figure 3: Comparison of the reference model to experimental nuclei spectra results not used in the optimization, see legends for details and text for explanation.

[3] N. Tomassetti, *The Astrophysical Journal Letters* **752**, L13 (2012).
[4] Y. Génolini, *et al.*, *Phys. Rev. Lett.* **119**, 241101 (2017).
[5] O. Fornieri, *et al.*, *Phys. Rev. D* **104**, 103013 (2021).
[6] S. Thoudam, J. R. Hörandel, *MNRAS* **435**, 2532 (2013).
[7] H. Wu, E.-S. Seo, V. Ptuskin, *PoS* **ICRC2021**, 155 (2021).
[8] O. Fornieri, D. Gaggero, D. Grasso, *JCAP* **2020**, 009 (2020).
[9] C. Evoli, *et al.*, *JCAP* **02**, 015 (2017).
[10] D. Gaggero, *et al.*, *Phys.Rev.Lett.* **111**, 021102 (2013).
[11] K. M. Ferrière, *Rev. Mod. Phys.* **73**, 1031 (2001).
[12] A. C. Cummings, *et al.*, *Astrophys.J.* **831**, 18 (2016).
[13] M. Aguilar, *et al.*, *Phys. Rev. Lett.* **114**, 171103 (2015).
[14] O. Adriani, *et al.*, *Phys. Rev. Lett.* **129**, 101102 (2022).
[15] M. Aguilar, *et al.*, *Phys. Rev. Lett.* **115**, 211101 (2015).
[16] O. Adriani, *et al.*, *Phys. Rev. Lett.* **125**, 251102 (2020).
[17] M. Aguilar, *et al.*, *Phys. Rev. Lett.* **123**, 181102 (2019).
[18] M. Aguilar, *et al.*, *Phys. Rev. Lett.* **117**, 231102 (2016).
[19] F. Nozzoli, C. Cernetti, *Universe* **7**, 183 (2021).
[20] I. Cholis, D. Hooper, T. Linden, *Phys. Rev. D* **93**, 043016 (2016).
[21] Q. An, *et al.*, *Sci. Adv.* **5**, eaax3793 (2019).
[22] F. Alemanno, *et al.*, *Phys. Rev. Lett.* **126**, 201102 (2021).
[23] O. Adriani, *et al.*, *Phys. Rev. Lett.* **130**, 171002 (2023).
[24] O. Adriani, *et al.*, *Phys. Rev. Lett.* **129**, 251103 (2022).
[25] M. Aguilar, *et al.*, *Phys. Rev. Lett.* **119**, 251101 (2017).
[26] O. Adriani, *et al.*, *Phys. Rev. Lett.* **126**, 241101 (2021).
[27] O. Adriani, *et al.*, *Phys. Rev. Lett.* **128**, 131103 (2022).
[28] M. Aguilar, *et al.*, *Phys. Rev. Lett.* **126**, 041104 (2021).